Intermodulation Distortion in Analog FM Troposcatter Systems

By E. D. SUNDE

(Manuscript received May 20, 1963)

In broadband transmission over troposcatter paths, selective fading will be encountered with resultant transmission impairments, depending on the modulation method. An analysis has been made in a companion paper of such selective fading, based on an idealized model of troposcatter paths. It indicated that selective fading will be accompanied by phase nonlinearity which in a first approximation can be regarded as quadratic over a narrow band. A probability distribution for such quadratic phase distortion was derived. On the premise of quadratic phase distortion, the error probability owing to selective fading was determined for digital transmission by various methods of carrier modulation.

The same idealized model and basic premise of quadratic phase distortion is used here to determine intermodulation distortion in FM for a signal with the statistical properties of random noise. An approximate expression for intermodulation noise owing to specified quadratic phase distortion has been derived, applying for any method of frequency preemphasis in FM. In turn, median intermodulation noise as well as the probability distribution of intermodulation noise has been determined, as related to certain basic system parameters.

A comparison is made of predicted with measured intermodulation noise in four troposcatter systems with lengths from 185 to 440 miles. The results indicate that phase nonlinearity owing to selective fading can be approximated by quadratic phase distortion, or linear delay distortion, over an appreciable part of the transmission band ordinarily considered for troposcatter systems, with a probability distribution that can be determined from certain basic parameters of troposcatter links, such as the length and antenna beam angles. However, to predict intermodulation distortion on any system, further experimental data than are now available are required on beam broadening by scatter.

The present random multipath FM distortion theory is shown to afford

a significant improvement over an equivalent single-echo theory that has been applied on an empirical basis to troposcatter systems.

INTRODUCTION

An analysis has been made elsewhere[1] of error probabilities in high-speed digital transmission over idealized troposcatter paths, considering both random noise and intersymbol interference owing to pulse distortion caused by selective fading. The above analysis indicated that a principal cause of intersymbol interference is a quadratic component of phase distortion, or linear delay distortion. On the same basic premise an evaluation is made herein of intermodulation noise in analog transmission by frequency modulation, as now used for transmission of voice channels in frequency division multiplex. Expressions and curves are given of intermodulation noise in an idealized troposcatter channel for a signal with the properties of random noise, as related to certain basic system parameters and comparisons are made with the results of measurements on four troposcatter systems.[2,3]

In random multipath transmission the received wave can be considered the sum of a plurality of echoes, arriving over the various paths with varying amplitudes and different delays. Although this view is conceptually simple, it does not facilitate analysis of the statistical properties of the received signal and of signal distortion. In the combination of a number of time functions, such as echoes, the analysis is greatly facilitated by the use of Fourier transformation to determine the corresponding spectra. The latter can in turn be combined directly with appropriate attention to phase relations to obtain the resultant wave. For this reason it is preferable from the standpoint of analysis to regard the received wave as a multiplicity of sine wave components, rather than signal wave echoes, arriving over the plurality of transmission paths with varying amplitudes and phases. This is the method ordinarily used in the analysis of the statistical properties of narrow-band random noise, which has properties that with appropriate translation of the basic parameters are also applicable to random multipath transmission. It is the method underlying both the previous determination of error probabilities in digital transmission owing to noise and selective fading, and the present analysis of intermodulation noise in FM.

In certain radio systems the received wave can be considered the sum of a principal signal wave and a weaker echo, and comprehensive theoretical analyses have been published of intermodulation noise in FM owing to such echo distortion,[4,5,6] together with the results of simulative tests.[7] For these reasons this two-path model has been adopted as a

coarse simile to multipath transmission in some interpretations of the result of measurements of intermodulation noise in troposcatter systems.[3] The limitations of this simile are recognized in the latter publication,[3] in which it is suggested that a more refined analysis is desirable. The idealized multipath model used in the analysis of troposcatter digital transmission affords a significant improvement, though it has certain predictable limitations, as shown herein.

I. TRANSMITTANCE PROPERTIES OF TROPOSCATTER LINKS

In tropospheric transmission beyond the horizon the received wave can be considered the sum of a large number of components of varying amplitudes resulting from a multiplicity of reflections within the common volume of the antennas. Owing to variations in the structure of the common volume, caused largely by winds, there will be relatively slow changes in the many reflections and thus in the amplitudes of the component waves. When a steady-state sine wave is transmitted, the received wave will thus exhibit random variations in its envelope and phase, known as fading.

In addition to such transmittance variations with time at a particular frequency, there will be transmittance variations with frequency at any given instant, as illustrated in Fig. 1. At a given instant the amplitude and phase characteristics of the transmission path may be as indicated in Fig. 1(a) and at a later instant as in Fig. 1(b).

Let $u = \omega - \omega_0$ represent the radian frequency relative to a reference frequency ω_0. When the transmission vs frequency characteristic of a troposcatter channel varies slowly with time t, it can be represented by

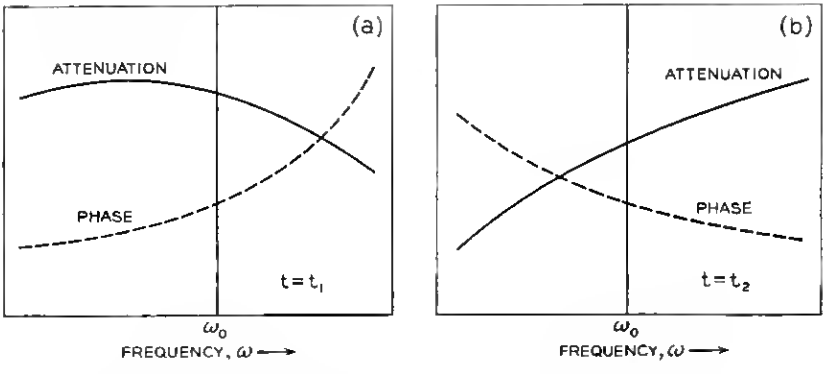

Fig. 1 — Illustrative variations in attenuation and phase characteristics with frequency at two instants t_1 and t_2.

$$T(u,t) = A(u,t)e^{-i\varphi(u,t)} \tag{1}$$

where

$A(u,t)$ = amplitude characteristic as a function of t for a fixed u, or as a function of u for a fixed time t

$\varphi(u,t)$ = phase characteristic.

If $u = u_0$ is fixed, both $A(u_0, t)$ and $\varphi(u_0, t)$ are random variables of the time t, as are the time derivatives $A'(u_0, t)$, $A''(u_0, t)$, $\varphi'(u_0, t)$, $\varphi''(u_0, t)$. The probability distributions of $A(u_0, t)$ and $\varphi(u_0, t)$ can be determined on the premise that they are the sum of a large number of randomly phased components. This results in a Rayleigh probability distribution of $A(u_0, t)$, in conformance with observations of rapid fading. To determine the probability distributions of A', A'', φ' and φ'', statistical information is required regarding the rapidity of fades. This ordinarily takes the form of the time autocorrelation functions of $A(t)$, or the related power spectrum of changes in transmittance amplitude. Such power spectra can be characterized by a certain equivalent fading bandwidth.

If the time is assumed fixed at $t = t_0$, then $A(u,t_0)$ and $\varphi(u,t_0)$ will have certain random fluctuations with the frequency u that can be characterized by probability distributions. This also applies to $\dot{A}(u,t_0)$, $\ddot{A}(u,t_0)$, $\dot{\varphi}(u,t_0)$, and $\ddot{\varphi}(u,t_0)$, where the dots indicate differentiation with respect to frequency u. The probability distributions of $\ddot{A}$, $\dot{\varphi}$, and $\dot{A}$ and $\ddot{\varphi}$ depend on the frequency autocorrelation functions, or the corresponding power spectra of variations with frequency. The latter depend on differences in transmission time over the various paths, and can be related to the maximum departure Δ from the mean transmission delay.

The amplitude and phase characteristics as a function of u at any time t_0 can in general be represented by a power series as

$$A(u,t_0) = a_0 + a_1u + a_2u^2 + a_3u^3 + \cdots \tag{2}$$

$$\varphi(u,t_0) = b_0 + b_1u + b_2u^2 + b_3u^3 + \cdots. \tag{3}$$

Certain basic relations have been developed by Carson and Fry[7] and by van der Pohl,[8] for transmission impairments in FM resulting from attenuation and phase distortion. With the aid of these relations it can be shown that intermodulation noise is caused principally by phase distortion rather than by amplitude distortion. Moreover, it can be shown that the principal contributor is quadratic phase distortion represented by b_2u^2, which correspouds to linear delay distortion $2b_2u$.

II. PROBABILITY DISTRIBUTION OF QUADRATIC PHASE DISTORTION

From (3) it follows that

$$\ddot{\varphi}(u,t_0) = 2b_2 + 6b_3u + \cdots. \tag{4}$$

For $u = 0$, i.e., at the reference or carrier frequency, the probability distribution of b_2 is the same as that of $\ddot{\varphi}(0,t)$. The latter probability distribution has been determined elsewhere[1] on the approximate premise of a linear variation in transmission delay, with maximum departures $\pm\Delta$ from the mean delay. In Fig. 2 is shown the probability that $\ddot{\varphi}$, or $2b_2$, exceeds $\Delta^2/3$ by a factor k. For example, there is a probability $p = 0.5$ that $\ddot{\varphi}$ exceeds $\Delta^2/3$ by a factor $k \approx 1.2$, and a probability $p = 0.1$ that $\ddot{\varphi}$ exceeds $\Delta^2/3$ by a factor $k \approx 19$.

Thus in general

$$\ddot{\varphi}_p = 2b_2(p) = k_p\Delta^2/3 \tag{5}$$

where $k_p\Delta^2/3$ is the value of $\ddot{\varphi}$, or $2b_2$ with a probability p of being exceeded.

Alternatively, the value of b_2 with a probability p of being exceeded is

$$b_2(p) = \frac{k_p}{6}\Delta^2. \tag{6}$$

Thus

$$b_2(0.5) \approx \frac{1.2}{6}\Delta^2 = 0.2\Delta^2 \tag{7}$$

$$b_2(0.1) \approx \frac{19}{6}\Delta^2 = 3.2\Delta^2 \tag{8}$$

$$b_2(0.01) \approx \frac{400}{6}\Delta^2 = 67\Delta^2. \tag{9}$$

Thus, when Δ is known, together with intermodulation noise for quadratic phase distortion, it is possible to determine the median value of average intermodulation noise, or the value exceeded with any other specified probability p.

III. INTERMODULATION NOISE FROM QUADRATIC PHASE DISTORTION

In a first-order evaluation of intermodulation noise, only the quadratic term b_2u^2 in (3) would be considered, since it will be the principal contributor. The ratio of nonlinear distortion power to average signal power at the frequency ω will depend on the signal properties and on the pre-

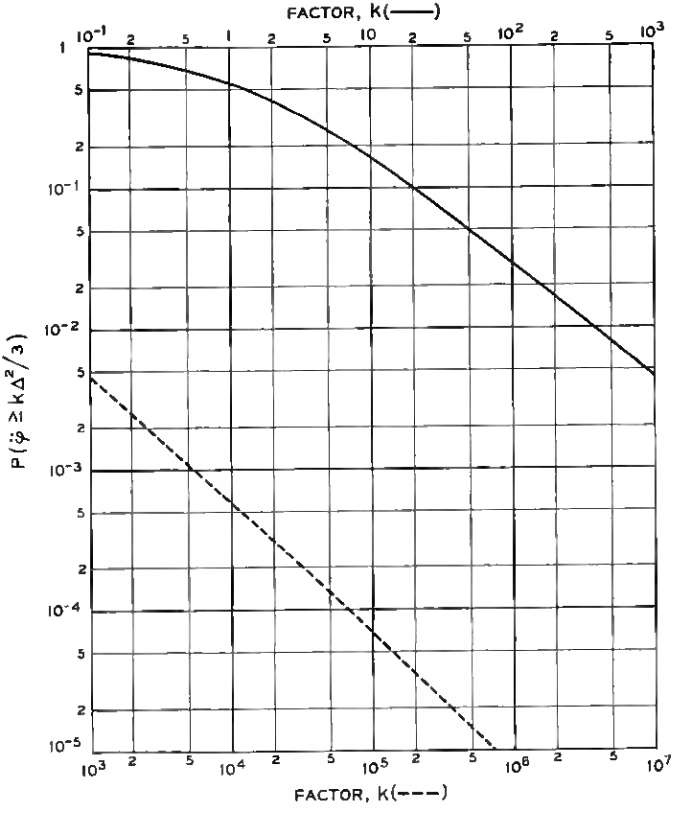

Fig. 2 — Probability that $\ddot{\varphi}$ or $2b_2$ exceeds $\Delta^2/3$ by a factor k.

emphasis used in frequency modulation. It will be assumed that the original message wave has a flat power spectrum of radian bandwidth $\Omega = 2\pi B$ and the statistical properties of random noise, and furthermore that the message wave is passed through a transmitting filter with a power transfer characteristic

$$\begin{aligned} t(\omega) &= 1 + c(\omega/\Omega)^2 \\ &= 1 + c(f/B)^2. \end{aligned} \tag{10}$$

At the receiving end a complementary filter is used to restore the message wave.

As discussed in the Appendix, exact determination of intermodulation noise from quadratic phase distortion presents formidable difficulties, except on the premise of slight phase distortion, which is not generally applicable to troposcatter systems. However, it is possible to obtain an

approximate solution without the above limitation. The following relation is derived in the Appendix for the ratio $\rho(f)$ of intermodulation noise to average signal power at the frequency $f = \omega/2\pi$

$$\rho(f) = \frac{B^2}{D^2} G(c,a) H(\gamma) \tag{11}$$

where c is defined by (10)

$$\begin{aligned} a &= f/B = \omega/\Omega \\ B &= \text{bandwidth of baseband signal} = \Omega/2\pi \\ D &= \text{rms frequency deviation} = \underline{\Omega}/2\pi \end{aligned}$$

and

$$\gamma = b_2\underline{\Omega}^2 = (2\pi)^2 b_2 D^2. \tag{12}$$

The function $G(c,a)$ depends on the pre-emphasis and is given by expression (108) in the Appendix, which is

$$\begin{aligned} G(c,a) &= \frac{3a^2}{(1 + ca^2)(3 + c)} F(c,a) \\ F(c,a) &= 2 - a + \frac{2c + c^2a^2}{3} [1 + (1 - a)^3] \\ &\quad - \frac{c^2 a}{2} [1 - (1 - a)^4] + \frac{c^5}{5} [1 + (1 - a)^5] \end{aligned} \tag{13}$$

This function is shown in Fig. 3 for pure FM and PM and for $c = 16$. The particular case of $c = 16$ and $a = 1$ will be considered further in the following, and for this case

$$G(16,1) = 0.192.$$

The function $H(\gamma)$ is shown in Fig. 4 and represents an approximation, as discussed in the Appendix. It will be noted that this function departs from proportionality with γ^2 for $\gamma \geqq 0.5$, reaches a certain maximum value and then diminishes.

IV. INTERMODULATION NOISE IN TROPOSCATTER PATHS

In accordance with (6), the value of b_2 with a probability p of being exceeded is $b_2(p) = k_p\Delta^2/6$. The corresponding value of γ is given by (12) as

$$\begin{aligned} \gamma_p &= \frac{k_p\Delta^2}{6} (2\pi)^2 D^2 \\ &= 6.6 k_p (\Delta D)^2. \end{aligned} \tag{14}$$

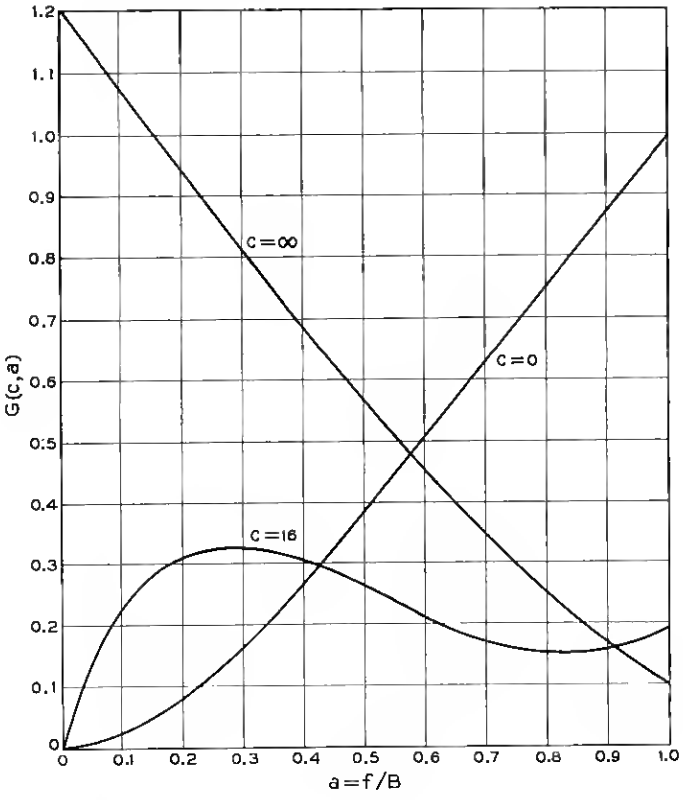

Fig. 3 — Function $G(c,a)$ for pure FM ($c = 0$), pure PM ($c = \infty$), and for pre-emphasized FM with $c = 16$.

Thus

$$\gamma_{0.5} \approx 8\ (\Delta D)^2 \tag{15}$$

$$\gamma_{0.1} \approx 125\ (\Delta D)^2 \tag{16}$$

$$\gamma_{0.01} = 2600\ (\Delta D^2). \tag{17}$$

The corresponding ratios $\rho(f)$ at $f = B$ with a probability p of being exceeded

$$\rho_p(B) = 0.192 \left(\frac{B}{D}\right)^2 H(\gamma_p) \tag{18}$$

$$\rho_{0.5}(B) = 0.192 \left(\frac{B}{D}\right)^2 H(8\Delta^2 D^2) \tag{19}$$

$$\rho_{0.1}(B) = 0.192 \left(\frac{B}{D}\right)^2 H(125\Delta^2 D^2) \tag{20}$$

$$\rho_{0.01}(B) = 0.192 \left(\frac{B}{D}\right)^2 H(2600\Delta D^2). \tag{21}$$

V. DIFFERENTIAL TRANSMISSION DELAY Δ

Exact determination of the equivalent maximum departure from the mean transmission delay requires consideration of the antenna beam patterns as affected by scattering. On the approximate basis of equivalent antenna beam angles α, it follows from the geometry indicated in Fig. 5 that

$$\Delta \approx \frac{L}{v} \frac{\alpha + \beta}{2} \left(\theta + \frac{\alpha + \beta}{2}\right) \tag{22}$$

where $\beta \leqq \alpha$, v is the velocity of propagation in free space, L is the length of the link, and

$$\theta = \frac{L}{2R} = \frac{L}{2R_0 K} \tag{23}$$

where R_0 is the radius of the earth and the factor K is ordinarily taken as 4/3.

The equivalent antenna beam angle α from midbeam to the 3-db loss point depends on the free-space beam angle α_0 and on the effect of scatter, which is related in a complex manner to α_0 and the length L, or alternatively θ. Narrow-beam antennas as now used in actual systems are loosely defined by $\alpha_0 \leqq 2\theta/3$. For these, $\alpha \approx \alpha_0$ on shorter links, while on longer links $\alpha > \alpha_0$ owing to beam-broadening by scatter. Analytical determination of α for longer links appears difficult, and only limited experimental data are available at present. For broad-beam antennas, $\alpha_0 \gg 2\theta/3$ and beam-broadening by scatter is in theory inappreciable.

By way of numerical example, let $L = 170$ miles and $K = 4/3$, in which case $\theta = 0.016$ radian. With $\alpha_0 = 0.004$ radian $\ll 2\theta/3$ it is permissible to take $\alpha = \alpha_0$. With $\beta = \alpha = \alpha_0$, (22) gives $\Delta = 0.08 \times 10^{-6}$ second.

The differential delay Δ in general varies with time and for narrow-beam antennas can be considered the sum of two components

$$\Delta(t) = \Delta_0 + \Delta_1(t) \tag{24}$$

where Δ_0 is a fixed component obtained from (22) by taking $\alpha = \alpha_0$, the free-space beam angles. The variable component $\Delta_1(t)$ depends on

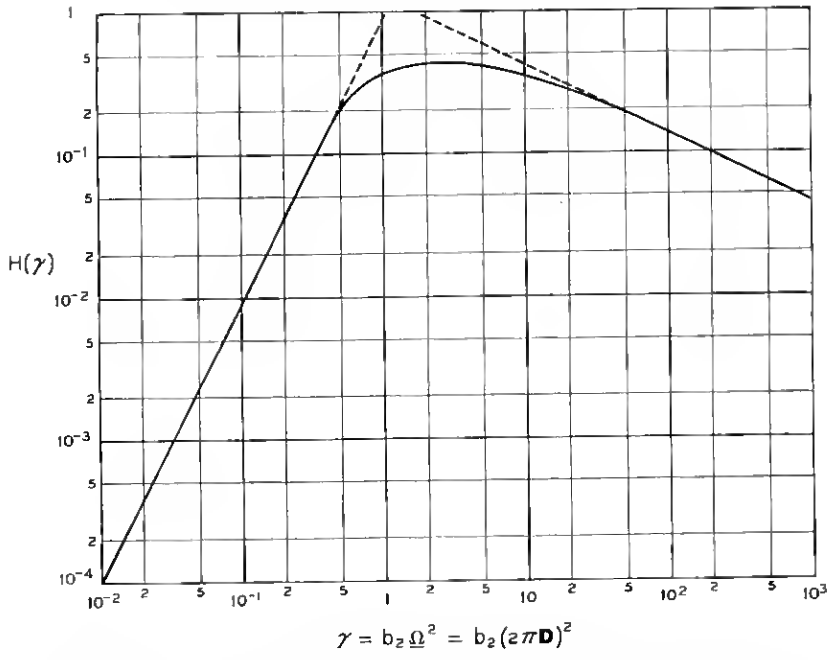

Fig. 4 — Function $H(\gamma)$. The parameter γ is the phase distortion in radians at a frequency corresponding to the rms frequency deviation $\Omega = 2\pi D$ radians/second.

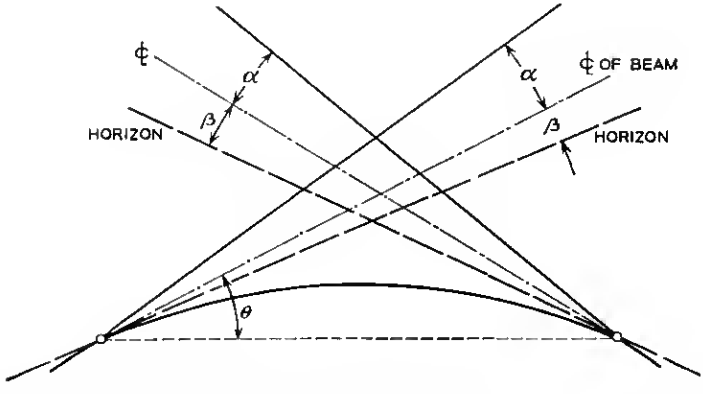

Fig. 5 — Definition of antenna beam angles α, take-off angle β and chord angle θ to midbeam. With different angles at the two ends, the mean angles are used in expressions for Δ.

scatter variation with time, as does path loss, and will have a certain correlation with path loss variations. Owing to the fixed component Δ_0, a weaker correlation exists between $\Delta(t)$ and path loss variations.

Because of the dependence of Δ on path loss, the ratio ρ_p of intermodulation noise to average signal power will depend somewhat on path loss However, for a given path loss ρ_p is independent of the average transmitter power and thus of the average signal power at the receiver.

VI. LIMITATIONS ON FIRST-ORDER DISTORTION THEORY

The above first-order approximation applies for sufficiently narrow signal bandwidths at the detector input such that terms in (3) of higher order than u^2 can be neglected. Results given by Rice for random variables (Section 3.4 of Ref. 10) indicate there is no correlation between $\ddot{\varphi}$ and $\dddot{\varphi}$, so that distortion owing to the term b_3u^3 will combine on a power addition basis with distortion resulting from b_2u^2. Moreover, there is a negative correlation factor between $\ddot{\varphi}$ and $\dddot{\varphi}$, so that on the average b_4 is negative whenever b_2 is positive, and conversely. Hence distortion produced by b_4u^4 will on the average subtract directly on an amplitude basis from that resulting from b_2u^2. In the range where the function $H(\gamma)$ increases linearly with γ^2, intermodulation noise owing to the term b_2u^2 increases as $b_2^2(\Delta D)^4$. In the same range, intermodulation noise from the term b_4u^4 will vary as $b_4^2(\Delta D)^8$ and may hence have a significant effect for adequately large values of ΔD even though b_4 be much smaller than b_2. As shown later, comparisons of measured intermodulation noise with predictions based on the above first-order theory indicate the increasing importance of the term b_4u^4 in reducing intermodulation noise as ΔD is increased.

VII. TWO-PATH VS MULTIPATH DISTORTION THEORY

The above first-order distortion theory is a mathematically derived approximation that in principle yields valid results with appropriate limitations on signal bandwidth and frequency deviation, and which retains the multipath feature that is essential to this end. By contrast, the two-path or single-echo simile mentioned in the introduction has no such basis but has been adopted principally because of the convenience of available theoretical analysis.[4,5,6] A second reason is that single-echo distortion theory yields results that in some respects are quite similar to those obtained with multipath transmission, as shown below.

It is noteworthy that, by proper choice of echo amplitude and delay, results similar to those for median quadratic phase distortion can be

obtained. This is illustrated in Fig. 6, which shows the median ratio $\rho(B)$ obtained from (19) as a function of D for $B = 1$ mc/sec with $\Delta = 0.1$ and 0.5 microsecond. In the same figures are shown the ratios $\rho(B)$ obtained on the premise that the received wave consists of a main signal and an echo of equal amplitude delayed by 0.07 and 0.4 microsecond. The ratio $\rho(B)$ for the latter condition is obtained from a chart given in Fig. 9 of Ref. 3, applying for FM with virtually the same pre-

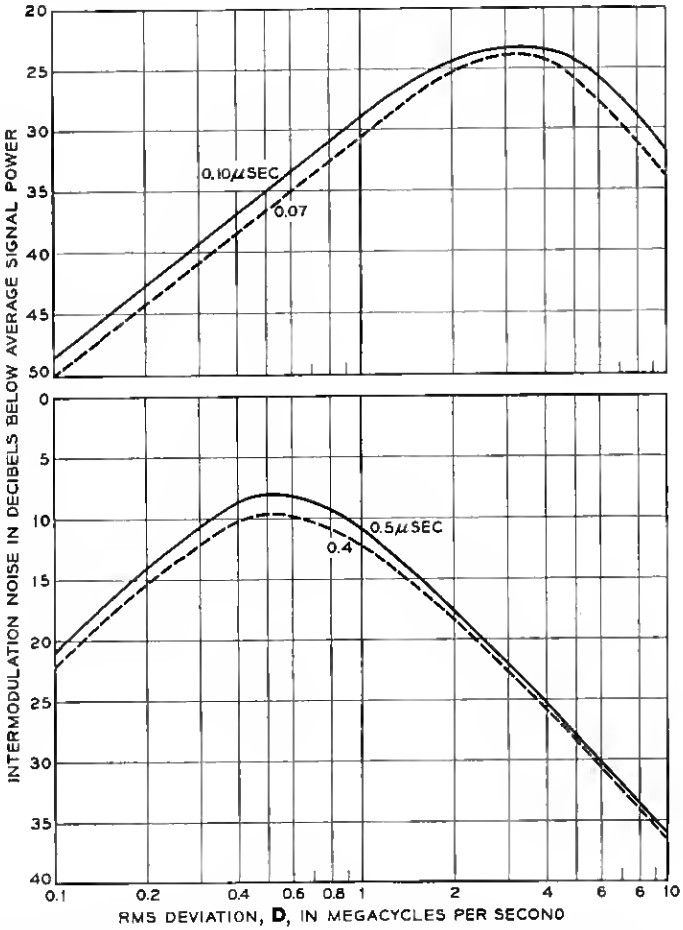

Fig. 6 — Comparison of intermodulation noise from single-echo distortion and quadratic phase distortion at $B = 1$ mc/sec: (solid lines) median intermodulation noise from quadratic phase distortion for indicated departures Δ from mean delay; (dashed lines) intermodulation noise from echo of same amplitude as signal with delays Δ_e as indicated.

emphasis as assumed herein and given by (10). The above charts are based on echo distortion theory applying for echoes that are much weaker than the signal, but this premise is ignored here in extending the theoretical results to a fictitious echo of the same amplitude as the signal. In this connection it may be noted that simulative tests[9] indicate that intermodulation noise is nearly proportional to echo amplitude, even when the latter equals the signal amplitude. With both quadratic phase distortion and single-echo distortion, intermodulation noise is virtually proportional to the second power of signal bandwidth. Hence, the relative comparisons in Fig. 6 could also apply for other bandwidths than $B = 1$ mc/sec.

The above comparisons indicate that in applying equivalent single-echo FM distortion theory to multipath transmission as in troposcatter systems, with physically tenable echo delays, certain dilemmas will be encountered. The theory could be extended beyond its validity to fictitious echoes of the same amplitude as the signal, to obtain virtually the same median intermodulation noise as for quadratic phase distortion. This would exclude the possibility of greater intermodulation noise than the median value, since the greater echo is by definition the main signal. The other procedure would be to assume an echo that is smaller than the main signal, which is physically more acceptable and does not violate the basic premise underlying echo distortion theory. In this case intermodulation noise predicted on the basis of echo distortion theory would, at least in certain cases, be much smaller than actually observed and could not be made to conform with observations, unless the echo amplitude is increased to the same amplitude as the signal.

Thus, if the ratio of echo amplitude to signal amplitude is r, intermodulation noise power based on single-echo theory will be less than for multipath transmission by a factor r^2. Hence it becomes necessary to introduce a factor $1/r^2$ to make single-echo theory applicable to multipath transmission. In Ref. 3, this factor has been determined empirically from measurements to be discussed later, and is given as 9 db.

VIII. OBSERVED MEDIAN INTERMODULATION NOISE

Measurements have been made on four troposcatter links of the median value of intermodulation noise at the frequency $f = B$. The modulating wave in these tests had a flat power spectrum, and pre-emphasis was used that closely corresponded to $c = 16$ in (10).

The basic parameters of the systems on which the measurements were made are given in Ref. 3 and are summarized in Table I. In this table α_0 is the free-space antenna beam angle from midbeam to the 3-db

TABLE I — BASIC PARAMETERS OF TROPOSCATTER TEST SYSTEMS IN CARIBBEAN (A) AND IN ARCTIC (B,C,D)

System	A	B	C	D
Length, miles	185	194	340	440
Radio frequency, mc	725	900	900	800
Antenna/diameter, ft	60, 60	30, 60	120, 120	120, 120
α_0 (radian)	0.0115	0.017	0.0058	0.0058
θ (radian)	0.015	0.016	0.031	0.034
Δ_0 (microsecond)	0.12	0.21	0.185	0.255

loss point, which may not conform with the angle α in (22) when scatter is considered. The values of K and θ are taken from Ref. 3, and θ differs slightly from that obtained from (23) owing to differences in antenna elevations. The take-off angle β is virtually zero and has been neglected. The value Δ_0 of Δ given in the table was calculated with $\alpha = \alpha_0$, rather than the actual beam angle with scatter. Systems A, B, C and D correspond to paths 1, 2, 4 and 3 in Ref. 3.

In Figs. 7 and 8 are shown the ratios ρ_1 (B) expressed in db as a function of the rms frequency deviation D for different bandwidths B of the baseband signals.

IX. COMPARISON OF THEORETICAL WITH OBSERVED MEDIAN VALUES

In the same Figs. 7 and 8 are shown median values of intermodulation noise obtained from (19) for each case, based on values Δ_m of Δ that afford the best average approximation to the measurements. The latter values are somewhat greater than Δ_0, as indicated in Table II.

A ratio Δ_m/Δ_0 or $\alpha_m/\alpha_0 > 1$ is to be expected owing to beam-broadening by scatter, and the above ratios appear reasonable in the light of present knowledge. Thus, if the actual angles α were known so that Δ could be determined, it appears plausible that satisfactory conformance with observed intermodulation noise would be obtained.

As noted in Section V, Δ includes a component $\Delta_1(t)$ that varies with time depending on scatter conditions and which is correlated with path loss fluctuations. The ratio ρ thus depends on path loss as affected by scatter and has a certain correlation with path loss variation, as shown elsewhere.[3] Hence, if measurements had been made under different path loss conditions, the derived values Δ_m would have been somewhat different.

From Figs. 7 and 8 it will be noted that with the above choice of $\Delta = \Delta_m$ it is possible to obtain better agreement between predicted and observed intermodulation noise for small bandwidths B of the baseband

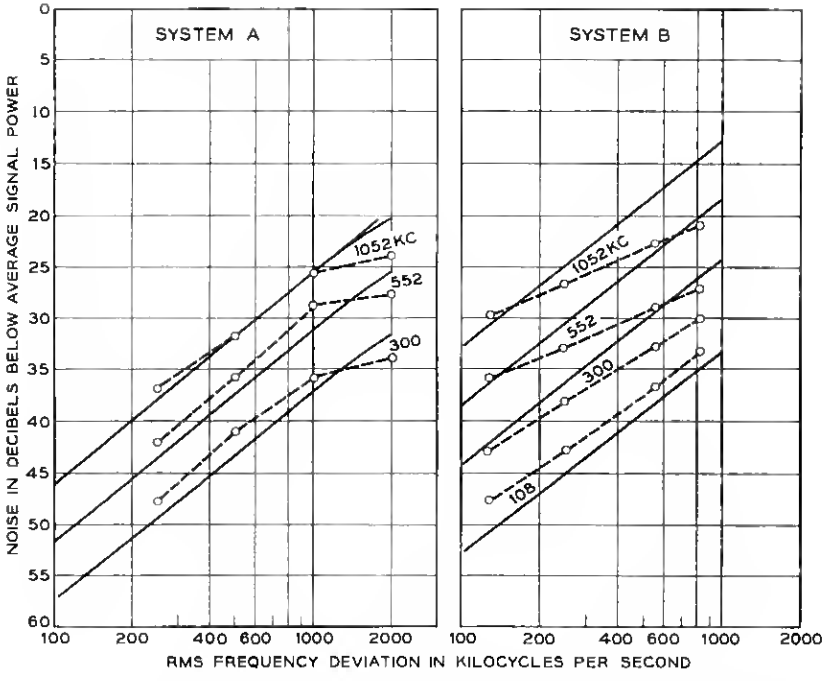

Fig. 7 — Comparison of measured and calculated median intermodulation noise: (dashed curves) measured median intermodulation noise in top channels at indicated frequencies in kc; (solid curves) calculated median intermodulation noise for idealized model with the following values of the equivalent maximum deviation Δ from the mean transmission delay: system A, $\Delta_m = 0.12$ microsecond ($\Delta_0 = 0.12$); system B, $\Delta_m = 0.25$ microsecond ($\Delta_0 = 0.12$).

signal and small deviations D than for large bandwidths and frequency deviations. This probably resides in the circumstance that the phase distortion terms of higher order than b_2u^2 have been neglected in the above first-order theory, as discussed in Section VI.

The measured median ratios given in Figs. 7 and 8 are plotted in Fig. 9 against the ratios predicted by first-order theory. It will be noted that measured intermodulation noise is less than predicted for signal-to-interference ratios less than about 30 db, owing to reduction in intermodulation noise by phase distortion of higher order than b_2u^2 that has been neglected in first-order theory. The results in Fig. 9 permit an approximate empirical correction to first-order theory.

As discussed in Section VII, with single-echo distortion theory virtually the same median intermodulation noise is obtained as with the above first-order theory, provided the echo is equal in amplitude to the

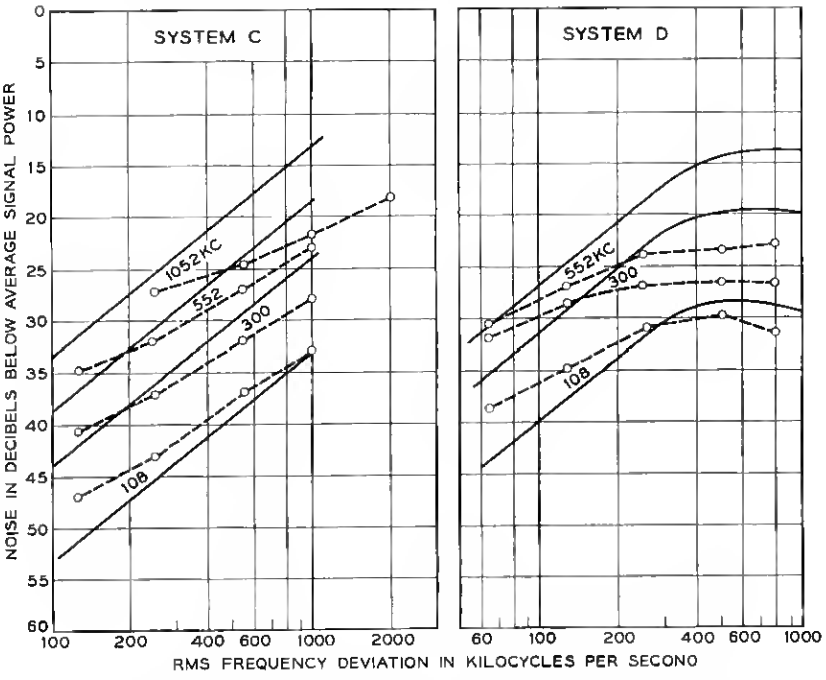

Fig. 8 — Comparison of measured and calculated median intermodulation noise: (dashed curves) measured median intermodulation noise in top channels at indicated frequencies in kc; (solid curves) calculated median intermodulation noise for idealized model with the following values of the equivalent maximum deviation Δ from the mean transmission delay: system C, $\Delta_m = 0.25$ microsecond ($\Delta_0 = 0.185$); system D, $\Delta_m = 0.55$ microsecond ($\Delta_0 = 0.255$).

mean signal. For smaller echoes, predicted intermodulation noise must be less. This conforms with results presented in Figs. 12 and 14 of Ref. 3, which show that intermodulation noise predicted from single-echo theory is significantly smaller than observed. To obtain a satisfactory average relation between predictions and observations, the predicted values must be increased by 9 db, as in Fig. 15 of Ref. 3

TABLE II — RATIO Δ_m/Δ_0

System	A	B	C	D
Length, miles	185	194	340	440
Δ_0, microsecond	0.12	0.21	0.185	0.255
Δ_m, microsecond	0.12	0.25	0.25	0.55
Δ_m/Δ_0	1.0	1.2	1.35	2.15
α_m/α_0	1.0	1.1	1.35	2.15

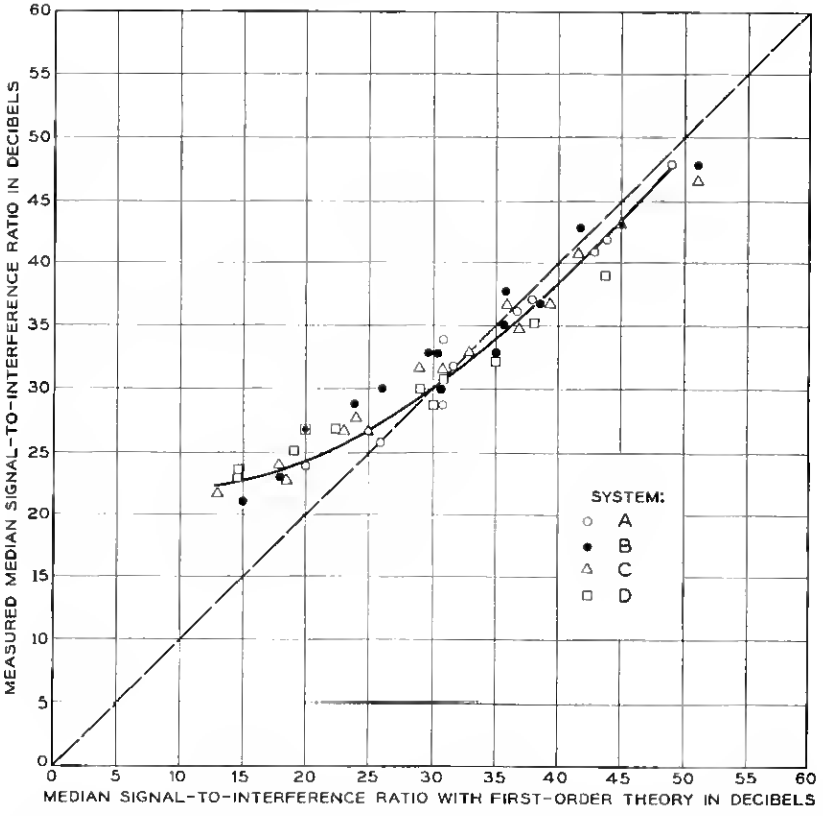

Fig. 9 — Comparison of measured median signal-to-interference ratios with median values based on first-order approximation with best choice of differential transmission delay Δ.

X. PROBABILITY DISTRIBUTION OF INTERMODULATION NOISE

From (18) it is apparent that the probability distribution of ρ is directly related to that of $H(\gamma_p)$. This function is shown in Fig. 10 as related to $(\Delta D)^2$ for $p = 0.5$, 0.1 and 0.01. It should be recognized that this function as given herein is approximate, and that the errors are likely to be greater for small values of p than for median intermodulation noise as considered previously.

From the curves in Fig. 10 it is possible to obtain approximate curves of the probability distribution of intermodulation noise, applying for various values of $\Delta^2 D^2$ as shown in Fig. 11. These curves show that the probability distributions vary markedly with the above parameter, in conformance with a few probability distributions derived from observa-

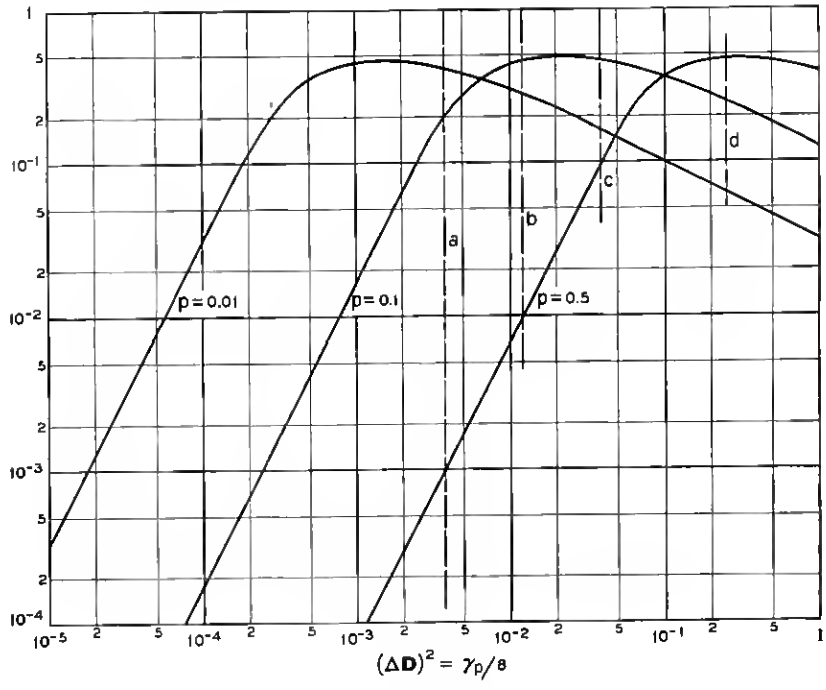

Fig. 10 — Function $H(\gamma_p)$ for various probabilities p.

tions.[2] Because of the approximations involved in the present first-order distortion theory, the above probability distribution curves should be considered illustrative and may not be accurate enough for certain engineering applications.

XI. PREDICTION OF INTERMODULATION DISTORTION

The present first-order intermodulation theory indicates that intermodulation distortion depends on the delay difference Δ, and this would apply also for an exact theory. For various troposcatter links with different angles α_0 and θ, intermodulation distortion would be the same for equal values of Δ. This is exemplified by comparison of intermodulation noise in systems B and C as shown in Figs. 7 and 8. Though these systems have different angles α_0 and θ, intermodulation noise is virtually the same since Δ is the same. Thus, if Δ could be determined, the above first-order theory, in conjunction with the above experimental data, would permit determination of intermodulation distortion for a variety

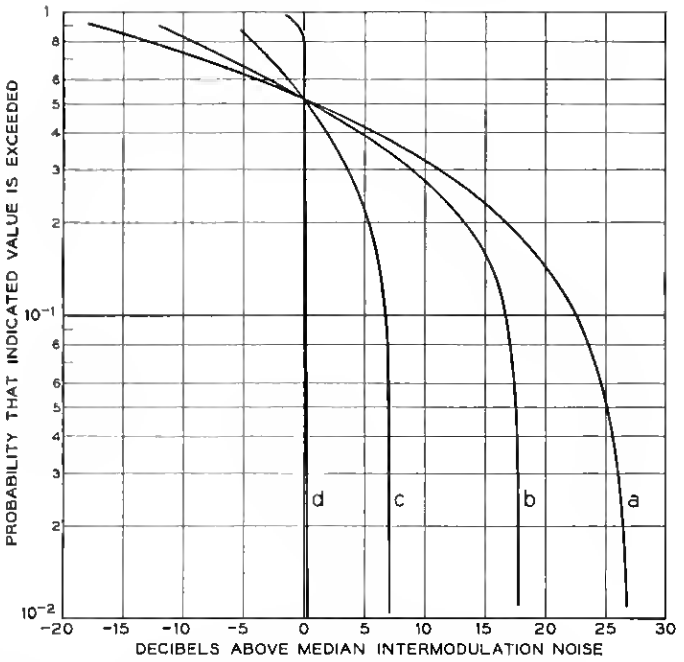

Fig. 11 — Probability distributions of intermodulation noise for various values of $(\Delta D)^2$ corresponding to dashed lines a, b, c and d in Fig. 10.

of conditions other than those in the tests. The above experimental data were confined to intermodulation noise in the top channel, i.e., for $a = 1$ in Fig. 3, and for a particular pre-emphasis, $c = 16$. The expression for $G(c,a)$, or the curves in Fig. 3, permit approximate determination of intermodulation noise at other frequencies, and also for other kinds of pre-emphasis. For example, for $a = 0.3$, intermodulation noise would be greater than for $a = 1$ by an approximate factor $0.32/0.19 \approx 1.7$. If pure FM($c = 0$) had been used in the tests, intermodulation noise at $a = 1$ would have been increased by an approximate factor $1/0.19 \approx 5.2$.

At present there is a principal obstacle to prediction of intermodulation distortion for other values of α_0 than in the above experimental systems. This is the lack of comprehensive experimental data on the beam angle α as affected by scatter for troposcatter links of various lengths. When and if such data become available, it will be possible to determine Δ and in turn intermodulation distortion in the manner indicated above for any kind of system.

XII. APPLICATION TO DIGITAL MULTIBAND TRANSMISSION

The distributions in Fig. 10 apply for average intermodulation noise over brief time intervals, as determined by changes in phase distortion with time. During each such interval the instantaneous amplitudes of intermodulation noise will fluctuate about the average value. For a signal with the properties of random noise, as considered here, the probability distribution of this fluctuation is approximated by the normal law. The distribution of instantaneous amplitudes or intermodulation noise is important in transmission by FM of a number of digital channels in frequency division multiplex, as discussed below.

In digital transmission over troposcatter paths, the error probability for a given signal-to-noise ratio of the receiver depends on the transmission rate, as discussed elsewhere.[1] As the transmission rate is increased, the error probability is ultimately determined by intersymbol interference owing to selective fading, and may be excessively high. The error probability can in this case be reduced, for a given total transmitter power, by transmitting at a slower rate over each of a number of narrower channels in frequency division multiplex. This could be accomplished by individual transmission over each channel, which would entail a number of independent transmitters. An alternative method would be to use a common amplifier and to transmit the combined digital signal by frequency modulation of a common carrier, as now used for transmission of voice frequency channels in frequency division multiplex. In the latter case, it is necessary to consider the possibility of additional transmission impairments owing to intermodulation noise.

With a sufficiently large number of digital channels in frequency division multiplex, the combined wave will have virtually a Gaussian amplitude distribution, like random noise. Hence the probability distribution of average intermodulation noise amplitudes would be as indicated in Fig. 11 for various conditions. The instantaneous amplitude will fluctuate with respect to the above average values, as noted in Section X.

In binary transmission it is often assumed that the error probability will not be excessive if the average noise power from all sources is about 12 db below the average signal power, or 18 db below the peak signal power in on-off binary pulse transmission. From the previous curves and expressions it appears that intermodulation noise power averaged over short intervals will be at least 10 db below the average signal power, with a small probability that it exceeds -15 db. It thus appears that intermodulation noise will not be a limiting or predominant factor even when a large number of binary channels are combined in frequency

division multiplex for transmission by frequency modulation of a common carrier.

XIII. SUMMARY

In broadband transmission over troposcatter paths, selective fading will be encountered with resultant transmission impairments, depending on the modulation method. A previous analysis has been made of such selective fading, based on an idealized model of a troposcatter path. It indicated that selective fading will be accompanied by phase distortion that in a first approximation can be regarded as quadratic, and a probability distribution curve for such quadratic phase distortion was derived. On the premise of such quadratic phase distortion, the error probability owing to selective fading was determined for digital transmission by various methods of carrier modulation.

In the present study the same basic premise of quadratic phase distortion has been used in determining intermodulation distortion for a signal with the properties of random noise, based on the same idealization of a troposcatter path. An approximate relation for intermodulation noise owing to quadratic phase distortion has been derived, applying for any frequency pre-emphasis in FM. In turn, median intermodulation noise as well as the probability distribution of intermodulation noise has been determined, as related to certain basic system parameters.

Median intermodulation noise predicted on basis of free-space antenna beam angles conforms well with observations on links 185 and 194 miles in length. For links 340 and 440 miles long it is necessary to use antenna beam angles that are greater than the free-space angles by factors of about 1.35 and 2.15, respectively. On long links employing narrow-beam antennas, beam broadening is expected because of scatter. Thus if the beam angles had been determined by independent observations or by more elaborate theory, it is probable that predicted intermodulation noise would conform reasonably well with observations.

The results of intermodulation noise measurements thus appear to confirm the conclusion in a previous theoretical analysis of troposcatter transmittance, which indicated that phase distortion owing to selective fading could in a first approximation be represented by a component of quadratic phase distortion, with a probability distribution that can be determined from certain basic system parameters. This affords a simplified first-order theoretical model of selective fading in troposcatter paths that is applicable to evaluation of resultant transmission impairments in both analog and digital transmission.

It can be shown analytically, and it is confirmed by observations, that the above first-order distortion theory yields intermodulation noise that in the case of large signal bandwidths and frequency deviations will be greater than observed or obtained with a more exact distortion theory. An empirical curve presented here permits determination of the expected correction for large bandwidths and frequency deviations.

It has also been demonstrated that the first-order multipath distortion theory presented here affords a significant improvement over single-echo distortion theory applied to random multipath transmission, in that it is simpler and accounts for the probability distribution of intermodulation noise without certain contradictions that are inherent in single-echo theory. Taken in conjunction with presently available data on observed intermodulation noise on certain troposcatter links, as discussed herein, it affords a means of predicting intermodulation noise on any system when more comprehensive experimental data become available on antenna beam broadening by scatter.

APPENDIX

Intermodulation Noise from Quadratic Phase Distortion in Pre-Emphasized FM

General

To facilitate analysis of intermodulation noise in FM owing to attenuation and phase distortion, it is customary to introduce two basic approximations. One is the use of "quasistationary theory" in conjunction with the concept of instantaneous frequency, which is permissible when the signal bandwidth B is negligible in comparison with the carrier frequency, so that the frequency changes imperceptibly over a signal interval $T = 1/2B$. The other customary approximation is that distortion $\alpha(\omega) + i\beta(\omega)$ is sufficiently small to permit the approximation $\exp [-\alpha(\omega) - i\beta(\omega)] \approx 1 - \alpha(\omega) - i\beta(\omega)$ over the bandwidth of the modulated carrier wave. The latter is a legitimate approximation for most transmission systems, and greatly simplifies the analysis, but may lead to appreciable errors in applications to tropospheric paths where pronounced attenuation and phase distortion can be encountered. For this reason an alternative approximate analysis is adopted herein to determine intermodulation noise from quadratic phase distortion, in which no limitation is placed on the phase distortion.

Two limiting cases are considered, from which it is possible to make an approximate determination of intermodulation noise as related to phase

distortion, rms frequency deviation, and bandwidth of the baseband signal. In the first case, phase distortion is assumed adequately small, such that the maximum phase distortion in the carrier signal band is less than π radians. Under this condition it is possible by use of "quasistationary" theory to determine the power spectrum of intermodulation noise without much difficulty. In the second case, no limitation is placed on phase distortion, in which case determination of the power spectrum becomes excessively difficult or laborious. It is possible, however, to determine total intermodulation noise power at the detector output, prior to post-detection low-pass filtering. From the manner in which total intermodulation noise power behaves with increasing phase distortion, it is possible to obtain an approximate evaluation of intermodulating noise in a narrow band, such as a voice channel.

A.1 *Power Spectrum of Phase Modulation*

In FM the transmitted wave is of the general form

$$V = \cos [\omega_0 t + \psi(t)] \tag{25}$$

where the phase $\psi(t)$ is related to the modulating wave $m(t)$ by

$$\psi(t) = k \int_0^t m(t)\, dt \tag{26}$$

where k is a constant.

The instantaneous frequency deviation is accordingly

$$\Omega(t) = \psi'(t) = km(t). \tag{27}$$

If the original signal wave has a power spectrum $s(\omega)$ and power preemphasis $p(\omega)$ is used, the power spectrum of the modulating wave is

$$W_m(\omega) = s(\omega)p(\omega). \tag{28}$$

The squared rms frequency deviation $\psi'(t)$ is

$$\underline{\Omega}^2 = k^2 \int_0^\infty s(\omega)p(\omega)\, d\omega. \tag{29}$$

In accordance with (26), $\psi(t)$ is the integral of $m(t)$. Hence the power spectrum of $\psi(t)$ is given by

$$W_\psi(\omega) = k^2 s(\omega)p(\omega)/\omega^2. \tag{30}$$

From (29) and (30)

$$W_\psi(\omega) = \underline{\Omega}^2 \frac{s(\omega)p(\omega)/\omega^2}{\displaystyle\int_0^\infty s(\omega)p(\omega)\, d\omega}. \tag{31}$$

The power spectrum of $\psi'(t)$ is $\omega^2 W_\psi(\omega)$.

A.2 *Autocorrelation Function of Phase Modulation*

The autocorrelation function of $\psi(t)$ is

$$R_\psi(\tau) = \int_0^\infty W_\psi(\omega) \cos \omega\tau \, d\omega \tag{32}$$

$$= k^2 \int_0^\infty \frac{s(\omega)p(\omega)}{\omega^2} \cos \omega\tau \, d\omega. \tag{33}$$

When the constant k is determined from (29), the following relation is obtained

$$R_\psi(\tau) = \underline{\Omega}^2 \left[\int_0^\infty \frac{s(\omega)p(\omega)}{\omega^2} \cos \omega\tau \, d\omega\right] \Big/ \left[\int_0^\infty s(\omega)p(\omega) \, d\omega\right]. \tag{34}$$

When the baseband power spectrum $s(\omega)$ has a bandwidth Ω, (34) can be written

$$R_\psi(\tau) = \mu^2 \left[\Omega^2 \int_0^\Omega \frac{s(\omega)p(\omega)}{\omega^2} \cos \omega\tau \, d\omega\right] \Big/ \left[\int_0^\Omega s(\omega)p(\omega) \, d\omega\right] \tag{35}$$

where μ is the rms deviation ratio

$$\mu = \underline{\Omega}/\Omega = D/B. \tag{36}$$

In the special case of a flat power spectrum, $s(\omega) = s$ and (35) yields

$$R_\psi(\tau) = \mu^2 \left[\Omega^2 \int_0^\Omega \frac{p(\omega)}{\omega^2} \cos \omega\tau \, d\omega\right] \Big/ \left[\int_0^\Omega p(\omega) \, d\omega\right]. \tag{37}$$

With pure FM, $p(\omega) = p =$ constant and (37) reduces to

$$R_\psi(\tau) = \mu^2 \int_0^1 \frac{\cos \Omega\tau x}{x^2} \, dx \tag{38}$$

where $x = \omega/\Omega$. From (38) it follows that

$$\begin{aligned} R_\psi(0) - R_\psi(\tau) &= \mu^2 \int_0^1 \frac{1 - \cos \Omega\tau x}{x^2} \, dx \\ &= \mu^2[\Omega\tau \, \mathrm{Si}(\Omega\tau) + \cos \Omega\tau - 1] \\ &= \mu^2 \frac{(\Omega\tau)^2}{2} \left[1 - \frac{(\Omega\tau)^2}{36} + \cdots\right] \end{aligned} \tag{39}$$

where Si is the sine integral function.

With pure PM, $p(\omega) = \omega^2$ and (37) yields

$$\begin{aligned} R_\psi(\tau) &= 3\mu^2 \int_0^1 \cos \Omega\tau x \, dx \\ &= 3\mu^2 \sin \Omega\tau/\Omega\tau \end{aligned} \tag{40}$$

$$R_\psi(0) - R_\psi(\tau) = 3\mu^2[1 - \sin \Omega\tau/\Omega\tau]$$
$$= \mu^2 \frac{(\Omega\tau)^2}{2}\left[1 - \frac{(\Omega\tau)^2}{20} + \cdots\right]. \tag{41}$$

A.3 *Intermodulation from Phase Distortion*

It will be assumed that the phase characteristic is of the form

$$\varphi(u) = b_0 + b_1 u + b_2 u^2 + b_3 u^3 + \cdots. \tag{42}$$

Phase distortion is then represented by the term

$$\beta(u) = b_2 u^2 + b_3 u^3 + \cdots \tag{43}$$

where $u = \omega - \omega_0$ is the frequency relative to the carrier frequency ω_0.

When the transmitted wave is of the form (25), the instantaneous frequency deviation is

$$u(t) = \psi'(t) \tag{44}$$

and the corresponding variation in phase distortion with time is

$$\beta[u(t)] = b_2[\psi'(t)]^2 + b_3[\psi'(t)]^3 + \cdots. \tag{45}$$

In the above relation $\psi'(t)$ is given by (27) and the power spectrum of $\psi'(t)$ by (28) multiplied by k^2 or

$$W_{\psi'}(u) = k^2 s(\omega) p(\omega). \tag{46}$$

In determining intermodulation distortion it must be recognized that distortion increases in the range $0 < \beta[u(t)] \leqq \pi$, diminishes in the range $\pi < \beta[u(t)] < 2\pi$, increases in the range $2\pi < \beta[u(t)] < 3\pi$, etc., as illustrated in Fig. 12.

To determine intermodulation distortion it is thus necessary to evaluate the distortion obtained when a wave with the power spectrum (46) is applied to a device with the output vs input characteristic illustrated in Fig. 12. Two limiting cases will be considered below.

A.4 *Intermodulation Spectrum for Small Quadratic Phase Distortion*

With quadratic phase distortion only, (45) becomes

$$\beta[u(t)] = b_2[\psi'(t)]^2. \tag{47}$$

It will be assumed that the probability that $\beta[u(t)]$ exceeds π is so small that it is permissible to assume $\beta[u(t)] < \pi$, and furthermore that $u(t)$ changes at a sufficiently slow rate such that $\beta'[u(t)] = 2b_2\psi''(t) \ll \pi$. For signals with the properties of random noise, these assumptions are

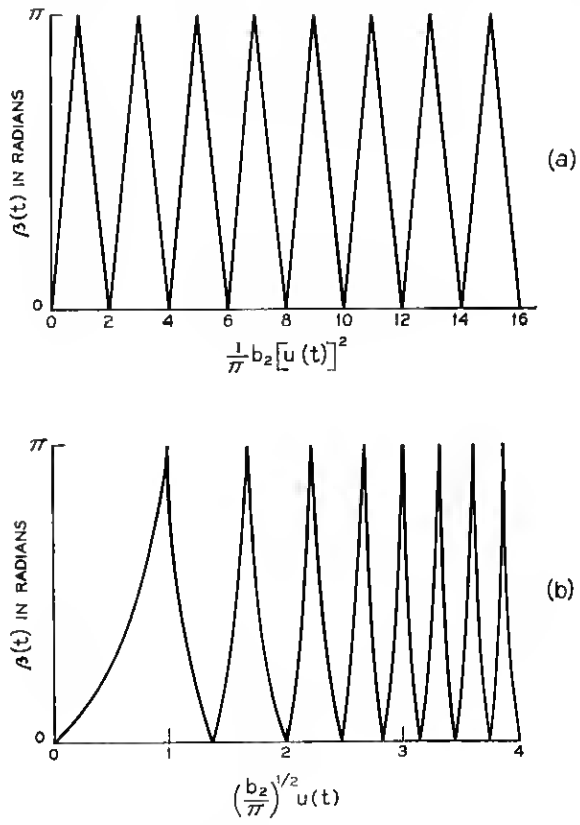

Fig. 12 — Instantaneous phase distortion $\beta(t)$ vs instantaneous frequency deviation $u(t)$ of signal.

permissible provided the rms phase error γ defined by (12) and appearing in Fig. 4 is much less than 1. With these assumptions, the autocorrelation function of the output phase distortion is the same as for a square law device and is given by (Ref. 10, Equation 4.10-1)

$$b_2^2[R_{\psi'}^2(0) + 2R_{\psi'}^2(\tau)]. \tag{48}$$

The first term can be identified with a dc component that does not give rise to noise. The power spectrum of the nonlinear output phase distortion is obtained from the second component in (48) and is given by

$$W_\psi^{(2)}(\omega) = 2b_2^2 \int_0^\infty R_{\psi'}^2(\tau) \cos \omega\tau \, d\tau. \tag{49}$$

The ratio of average intermodulation noise power at the frequency ω to the average signal power becomes

$$\rho(\omega) = \frac{W_\psi^{(2)}(\omega)}{W_\psi(\omega)} = \frac{2b_2^2 \int_0^1 R_{\psi'}^2(\tau) \cos \omega\tau \, d\tau}{k^2 p(\omega) s(\omega)/\omega^2}. \tag{50}$$

In view of (46) the following relation applies

$$R_{\psi'}(\tau) = k^2 \int_0^\infty s(\omega) p(\omega) \cos \omega\tau \, d\omega. \tag{51}$$

Expression (50) can be written

$$\rho(\omega) = \frac{2b_2^2 k^4 \int_0^\infty k^{-4} R_{\psi'}^2(\tau) \cos \omega\tau \, d\tau}{k^2 p(\omega) s(\omega)/\omega^2} \tag{52}$$

$$= \frac{2\gamma^2 a^2}{\mu^2} \frac{\int_0^\infty k^{-4} R_{\psi'}^2(\tau) \cos \omega\tau \, d\tau}{p(\omega) s(\omega) \int_0^\infty s(\omega) p(\omega) \, d\omega} \tag{53}$$

where

$$a = \omega/\Omega = f/B \tag{54}$$

$$\gamma = b_2 \mu^2 \Omega^2 = b_2 \Omega^2 = (2\pi)^2 b_2 D^2. \tag{55}$$

The following relation applies*

$$\int_0^\infty R_{\psi'}^2(\tau) \cos \omega\tau \, d\tau = \frac{1}{2} \int_0^\infty W_{\psi'}(u) W_{\psi'}(\omega - u) \, du \tag{56}$$

where $W_{\psi'}(u)$ is the power spectrum given by (46).

In view of (56) and (46), expression (53) can be written

$$\rho(\omega) = \frac{a^2\gamma^2/\mu^2}{p(\omega) s(\omega) \int_0^\infty p(\omega) s(\omega) d\omega} \cdot \int_{-\infty}^\infty s(\omega) p(\omega) s(\omega - u) p(\omega - u) du. \tag{57}$$

In the special case of a flat power spectrum $s(\omega) = s$ of bandwidth

* Ref. 10, Eq. (4C-6). In this reference the autocorrelation function is defined differently from the definition used here and has a factor 4 in integral (51), so that an additional factor $\frac{1}{4}$ appears in (56).

$\Omega = 2\pi B$, (57) becomes

$$\rho(\omega) = \frac{a^2\gamma^2/\mu^2}{p(\omega)\,\frac{1}{\Omega}\int_0^{\Omega} p(\omega)d\omega}\,\frac{1}{\Omega}\int_{\omega-\Omega}^{\Omega} p(u)p(\omega - u)du \tag{58}$$

$$= \frac{\gamma^2}{\mu^2}\,\frac{a^2}{p(a)\int_0^1 p(x)dx}\int_{a-1}^{1} p(x)p(a - x)dx. \tag{59}$$

When $p(x)$ is of the form

$$p(x) = 1 + c(u/\Omega)^2 = 1 + cx^2 \tag{60}$$

relation (59) becomes

$$\begin{aligned}\rho(\omega) &= \frac{3a^2\gamma^2}{\mu^2(1 + ca^2)(3 + c)}\int_{a-1}^{1}(1 + cx^2)[1 + c(a - x)^2]dx \\ &= \frac{\gamma^2 3a^2}{\mu^2(1 + ca^2)(3 + c)}F(c,a)\end{aligned} \tag{61}$$

where

$$\begin{aligned}F(c,a) = 2 - a + \frac{2c + c^2a^2}{3}[1 + (1 - a)^3] \\ - \frac{c^2a}{2}[1 - (1 - a)^4] + \frac{c^2}{5}[1 + (1 - a)^5].\end{aligned} \tag{62}$$

In the particular case of pure FM, $c = 0$ and $F(c,a) = 2 - a$, so that (61) yields

$$\begin{aligned}\rho(\omega) &= \frac{\gamma^2a^2}{\mu^2}(2 - a) \\ &= \left(\frac{B}{D}\right)^2\gamma^2a^2(2 - a)\end{aligned} \tag{63}$$

where $a = \omega/\Omega = f/B$, $D = \Omega/2\pi$ and $\gamma = b_2\Omega^2 = b_2(2\pi D)^2$.

The above result (63) conforms with an expression derived by Rice for this limiting case (Ref. 11, Equation 5.6).

A.5 *Total Intermodulation from Quadratic Phase Distortion*

The previous analysis of the power spectrum of intermodulation noise was based on the assumption that the maximum phase distortion in the transmission band is substantially less than 180°. Without this limitation, numerical determination of the power spectrum becomes very diffi-

cult, though a formal solution may be feasible. However, it is possible to determine total intermodulation distortion without too much difficulty, without limitation on the phase distortion, as shown below.

Let x designate the instantaneous amplitude of $\psi'(t) = km(t)$, and let x have a probability density

$$p(x) = \left(\frac{2}{\pi\sigma_x^2}\right)^{\frac{1}{2}} \exp\ (-x^2/2\sigma_x^2). \tag{64}$$

For large instantaneous frequency deviations $\psi'(t)$ the derivative $\psi''(t)$ is on the average sufficiently small to be neglected. The total intermodulation distortion in the received signal prior to post-detection low-pass filtering is then for a nonlinear characteristic as illustrated in Fig. 12.

$$\begin{aligned} I = &\int_0^{L_1} (b_2x^2)^2 p(x)dx + \int_{L_1}^{L_3} (2\pi - b_2x^2)^2 p(x)dx \\ &+ \int_{L_3}^{L_5} (4\pi - b_2x^2)^2 p(x)dx + \cdots + \int_{L_{2m-1}}^{L_{2m+1}} (2\pi m - b_2x^2)^2 p(x)dx \end{aligned} \tag{65}$$

where

$$L_j = (j\pi/b_2)^{\frac{1}{2}}.$$

With $b_2x^2 = u^2$, $\gamma = b_2\sigma_x^2$ and

$$p(u) = \left(\frac{2}{\pi\gamma}\right)^{\frac{1}{2}} \exp\ (-u^2/2\gamma) \tag{66}$$

expression (65) can be written

$$\begin{aligned} I = &\int_0^{l_1} u^4 p(u)du + \int_{l_1}^{l_3} (2\pi - u^2)^2 p(u)du \\ &+ \int_{l_3}^{l_5} (4\pi - u^2)^2 p(u)du + \cdots \end{aligned} \tag{67}$$

where

$$l_j = (j\pi)^{\frac{1}{2}}. \tag{68}$$

Writing $2m\pi - u^2 = -\tau$, $2u\,du = d\tau$, expression (67) can be transformed into

$$\begin{aligned} I = &\int_0^{\pi} \tau^{\frac{1}{2}} p(\tau)d\tau + e^{-\pi/\gamma} \int_{-\pi}^{\pi} \frac{\tau^2}{(2\pi + \tau)^{\frac{1}{2}}}\, p(\tau)d\tau \\ &+ e^{-2\pi/\gamma} \int_{-\pi}^{\pi} \frac{\tau^2}{(4\pi + \tau)^{\frac{1}{2}}}\, p(\tau)d\tau + \cdots \end{aligned} \tag{69}$$

where

$$p(\tau) = \left(\frac{1}{2\pi\gamma}\right)^{\frac{1}{2}} e^{-\tau/2\gamma}. \tag{70}$$

Total distortion I includes a mean or dc power component I_0 that must be subtracted from I to obtain the nonlinear component. The mean amplitude component $I_0^{\frac{1}{2}}$ is given by

$$I_0^{\frac{1}{2}} = \int_0^{L_1} b_2 x^2 p(x)dx + \int_{L_1}^{L_2} (2\pi - b_2 x^2)p(x)dx + \int_{L_3}^{L_5} (4\pi - b_2 x^2)p(x)dx + \cdots \tag{71}$$

where L_m and $p(x)$ are defined as before.

With the same notation as before, (71) can be transformed into

$$I_0^{\frac{1}{2}} = \int_0^{\pi} \tau^{\frac{1}{2}} p(\tau)d\tau + e^{-\pi/\gamma} \int_{-\pi}^{\pi} \frac{|\tau|}{(2\pi + \tau)^{\frac{1}{2}}} p(\tau)dt + e^{-2\pi/\gamma} \int_{-\pi}^{\pi} \frac{|\tau|}{(4\pi + \tau)^{\frac{1}{2}}} p(\tau)d\tau + \cdots . \tag{72}$$

In the above relations γ is the phase distortion corresponding to the rms frequency deviation as given by

$$\gamma = b_2\sigma_x^2 = b_2\underline{\Omega}^2 = b_2\mu^2\Omega^2. \tag{73}$$

The last relations follow from (29) since σ_x^2 is the variance of $\psi'(t)$.

The total average signal power is

$$S = R_\psi(0) = \mu^2 \left[\Omega^2 \int_0^{\Omega} \frac{p(\omega)}{\omega^2} d\omega\right] \Big/ \left[\int_0^{\Omega} p(\omega)d\omega\right] = \mu^2/C \tag{74}$$

where C is a constant depending on $p(\omega)$.

The ratio of total nonlinear intermodulation noise to total average signal power becomes

$$\rho = \frac{I - I_0}{S} = C\frac{I - I_0}{\mu^2} = C(I - I_0)\left(\frac{B}{D}\right)^2. \tag{75}$$

A.6 *Total Intermodulation for Small Phase Distortion*

For sufficiently small values of $\gamma = b_2\underline{\Omega}^2$, such that $\pi/\gamma \gg 1$, only the

first integral in (69) needs to be considered. Hence

$$I \approx \int_0^{\pi} \tau^{\frac{1}{2}} p(\tau) d\tau$$
$$= 3\gamma^2 \text{ erf } (z) - 3 \cdot 2^{\frac{1}{2}} \gamma^{\frac{1}{2}} \exp(-z^2) - 2^{\frac{1}{2}} \pi \gamma^{\frac{1}{2}} \exp(z^2) \quad (76)$$

where

$$z^2 = \pi/2\gamma. \quad (77)$$

With a similar approximation (72) yields

$$I_0^{\frac{1}{2}} \approx \int_0^{\pi} \tau^{\frac{1}{2}} p(\tau) d\tau \quad (78)$$
$$= \gamma \text{ erf } (z) - 2^{\frac{1}{2}} \exp(-z^2).$$

For $z \geqq 2$, or $\gamma \leqq \pi/8$:

$$I \approx 3\gamma^2 \quad \text{and} \quad I_0^{\frac{1}{2}} = \gamma.$$

Hence $I - I_0 = 2\gamma^2$ and (75) becomes

$$\rho = C \cdot 2 \frac{\gamma^2}{\mu^2} \quad (79)$$

where the constant C is defined through (74).

It will be noted that (79) is of the same basic form as (61) for the ratio $\rho(\omega)$ at the frequency ω. In (61) the multiplier of γ^2/μ^2 is a constant, as is the case in (79).

A.7 *Total Intermodulation for Large Phase Distortion*

When $\gamma \gg 1$, it is permissible to approximate $p(\tau)$ as given by (70) with

$$p(\tau) \approx \left(\frac{1}{2\pi\gamma}\right)^{\frac{1}{2}}. \quad (80)$$

This approximation is valid in evaluation of the various integrals in (69) and (72) provided that for the minimum value of $\tau = \pi$, $\exp(-\tau/2\gamma) \ll 1$. This is the case if

$$\pi/2\gamma \ll 1 \quad \text{or} \quad \gamma \gg \pi/2.$$

With (80) in (69)

$$I = \left(\frac{1}{2\pi\gamma}\right)^{\frac{1}{2}} \left[\int_0^{\pi} \tau^{\frac{1}{2}} d\tau + \sum_{m=1}^{\infty} e^{-m\pi/\gamma} \int_{-\pi}^{\pi} \frac{\tau^2 d\tau}{(2\pi m + \tau)^{\frac{1}{2}}}\right]. \quad (81)$$

In (81),

$$\int_{-\pi}^{\pi} \frac{\tau^2 d\tau}{(2m\pi + \tau)^{\frac{1}{2}}} = \frac{2 \cdot \pi^{\frac{5}{2}}}{15} [(2m + 1)^{\frac{1}{2}}(32m^2 - 8m + 3) - (2m + 1)^{\frac{1}{2}}(32m^2 + 8m + 3)] \tag{82}$$

$$\approx \frac{1}{m^{\frac{1}{2}}} \frac{2^{\frac{1}{2}}\pi^{\frac{5}{2}}}{3} \quad \text{for} \quad m \geqq 1 . \tag{83}$$

For $m = 1$, (82) gives about 0.5 and (83) about 0.47. Hence (83) represents a good approximation of (82).

With (83) in (81)

$$I = \left(\frac{1}{2\pi\gamma}\right)^{\frac{1}{2}} \left[\int_0^{\pi} \tau^{\frac{1}{2}}\, d\tau + \frac{2^{\frac{1}{2}}\pi^{\frac{5}{2}}}{3} \sum_{m=1}^{\infty} \frac{e^{-m\pi/\gamma}}{m^{\frac{1}{2}}}\right]. \tag{84}$$

As a first approximation the summation can be replaced by an integral, in which case

$$I \approx \left(\frac{1}{2\pi\gamma}\right)^{\frac{1}{2}} \left[\frac{2}{5}\pi^{\frac{5}{2}} + \frac{2^{\frac{1}{2}}\pi^{\frac{5}{2}}}{3} \int_{m=1}^{\infty} \frac{e^{-m\pi/\gamma}\, dm}{m^{\frac{1}{2}}}\right]. \tag{85}$$

With $m = u^2$

$$I = \left(\frac{1}{2\pi\gamma}\right)^{\frac{1}{2}} \pi^{\frac{5}{2}} \left[\frac{2}{5} + \frac{2^{\frac{1}{2}} \cdot 2}{3} \int_{u=1}^{\infty} e^{-u^2\pi/\gamma}\, du\right]$$

$$= \left(\frac{1}{2\pi\gamma}\right)^{\frac{1}{2}} \pi^{\frac{5}{2}} \left[\frac{2}{5} + \frac{2^{\frac{1}{2}}\gamma^{\frac{1}{2}}}{3} \operatorname{erfc}\left(\sqrt{\frac{\pi}{\gamma}}\right)\right] \tag{86}$$

$$= \frac{\pi^2}{3}\left[\operatorname{erfc}\left(\sqrt{\frac{\pi}{\gamma}}\right) + \frac{6}{5 \cdot 2^{\frac{1}{2}}\gamma^{\frac{1}{2}}}\right] \tag{87}$$

$$\approx \frac{\pi^2}{3} \quad \text{for} \quad \gamma \gg 4\pi . \tag{88}$$

By a similar approximation $I_0^{\frac{1}{2}}$ as given by (72) becomes

$$I_0^{\frac{1}{2}} = \left(\frac{1}{2\pi\gamma}\right)^{\frac{1}{2}} \left[\int_0^{\pi} \tau^{\frac{1}{2}}\, d\tau + \sum_{m=1}^{\infty} e^{-m\pi/\gamma} \int_{-\pi}^{\pi} \frac{|\tau|\, d\tau}{(2m\pi + \tau)^{\frac{1}{2}}}\right] \tag{89}$$

$$= \left(\frac{1}{2\pi\gamma}\right)^{\frac{1}{2}} \left[\frac{2}{3}\pi^{\frac{3}{2}} + \frac{\pi\sigma}{2^{\frac{1}{2}}} \operatorname{erfc}\left(\sqrt{\frac{\pi}{\gamma}}\right)\right] \tag{90}$$

$$= \frac{\sqrt{\pi}}{2}\left[\operatorname{erfc}\left(\sqrt{\frac{\pi}{\gamma}}\right) + \frac{2^{\frac{1}{2}}}{3\gamma^{\frac{1}{2}}}\pi^{\frac{1}{2}}\right] \tag{91}$$

$$\approx \frac{\pi^{\frac{1}{2}}}{2} \quad \text{for} \quad \gamma \gg 4\pi . \tag{92}$$

The ratio ρ is obtained from (75) with I as given by (87) and $I_0^{\frac{1}{2}}$ by (91). In the limit of $\gamma \to \infty$ the ratio becomes

$$\begin{aligned} \rho &= C \frac{I - I_0}{\mu^2} = \frac{C}{\mu^2} \pi \left(\frac{\pi}{3} - \frac{1}{4} \right) \\ &\approx 2.5 \frac{C}{\mu^2}. \end{aligned} \tag{93}$$

A.8 *Approximation for Total Intermodulation*

The general expression for the ratio ρ of total intermodulation noise power to average signal power can be written in the form

$$\rho = \frac{2C}{\mu^2} h(\gamma). \tag{94}$$

For the limiting case of $\gamma \to 0$, the function h is in accordance with (79)

$$h = \gamma^2. \tag{95}$$

For the other limiting case in which $\gamma \to \infty$, the function h is in accordance with (93)

$$h = 2.5/2 = 1.25. \tag{96}$$

In Fig. 13 are shown the above two limiting cases, together with the function h obtained from (75) as $\eta = I - I_0$, when I and I_0 are determined from (86) and (91). The approximate function $h(\gamma)$ is obtained by drawing a transition curve between the above two limiting cases, as in Fig. 13.

A.9 *Approximation for Intermodulation Spectrum*

The function $h(\gamma)$ in Fig. 13 is proportional to the total intermodulation noise power and can be related to the power spectrum $W_i(\omega)$ of intermodulation noise by

$$h(\gamma) = c_0 \int_0^\infty W_i(\omega)\, d\omega \tag{97}$$

where c_0 is a constant. Relation (94) can thus be written

$$\rho = \frac{2c_0 C}{\mu^2} \int_0^\infty W_i(\omega)\, d\omega. \tag{98}$$

For $\gamma \to 0$, (98) must conform with (95), which is possible provided the power spectrum is of the general form

$$W_i^0(\omega) = c_1\gamma^2 \frac{1}{\Omega} F_0(\omega/\Omega) \tag{99}$$

where F_0 is any functional relation dependent only on the ratio $a = \omega/\Omega$.

With (99) in (98)

$$\begin{aligned} \rho &= \frac{\gamma^2}{\mu^2} 2c_0c_1C \frac{1}{\Omega} \int_0^\infty F_0(\omega/\Omega)\, d\omega \\ &= \frac{\gamma^2}{\mu^2} 2c_0c_1C \int_0^\infty F_0(u)\, du. \end{aligned} \tag{100}$$

This yields relation (95) provided

$$c_0c_1C \int_0^\infty F_0(u)\, du = 1. \tag{101}$$

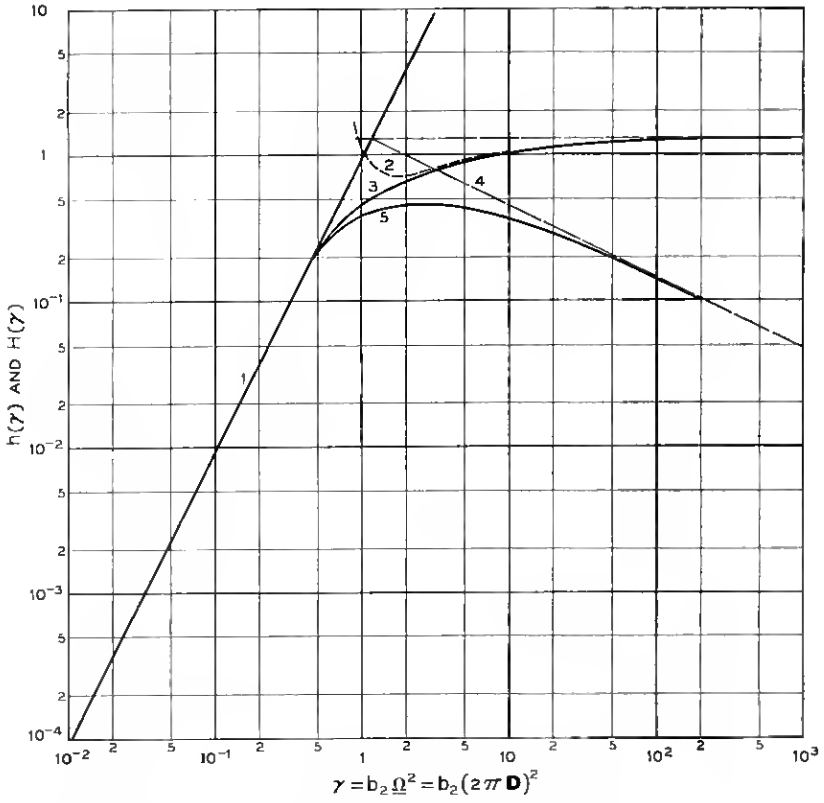

Fig. 13 — Functions $h(\gamma)$ and $H(\gamma)$: 1, functions $h(\gamma)$ and $H(\gamma)$ for $\gamma \ll 1$; 2, function $h(\gamma)$ for $\gamma \gg 1$; 3, approximate interpolated function $h(\gamma)$; 4, function $H(\gamma)$ for $\gamma \gg 1$; 5, approximate interpolated function $H(\gamma)$.

From (100) it is apparent that the ratio of intermodulation noise power to average signal power in a narrow band $d\omega$ at ω is

$$\rho(\omega) = \frac{\gamma^2}{\mu^2} 2c_0c_1C \frac{1}{\Omega} F_0(\omega/\Omega). \tag{102}$$

Comparison of (102) with (61) shows that in this case

$$2c_0c_1C \frac{1}{\Omega} F_0(\omega/\Omega) = \frac{3a^2}{(1 + ca^2)(3 + c)} F(c,a) \tag{103}$$

where $F(c,a)$ is given by (62).

In summary, for $\gamma \to 0$ the power spectrum has a fixed shape independent of γ and an amplitude proportional to γ^2.

Consider next the limiting case in which $\gamma \to \infty$. In accordance with (96) h theu approaches a constant, which is possible for various power spectra of the general form

$$W_i^{(\infty)}(\omega) = \frac{c_1}{\gamma^n} F_\infty(\omega/\gamma^n) \tag{104}$$

where $F_\infty(\omega/\gamma^n)$ is any functional relation dependent only on the ratio (ω/γ^n). In this case (104) in (98) yields

$$\begin{aligned} \rho &= \frac{2c_0c_1C}{\mu^2} \frac{1}{\gamma^n} \int_0^\infty F_\infty(\omega/\gamma^n)\, d\omega \\ &= \frac{2c_0c_1C}{\mu^2} \int_0^\infty F(u)\, du \end{aligned} \tag{105}$$

where $u = \omega/\gamma^n$.

The exponent n can be determined from consideration of the input vs output characteristic shown in Fig. 12. If b_2 is increased by a factor k, the intervals between zero points are multiplied by a factor $k^{-\frac{1}{2}}$, as indicated in Fig. 14 for $k = 4$. For a given frequency deviation, the bandwidth of the power spectrum is then multiplied by a factor $k^{\frac{1}{2}}$ and the amplitude of the spectrum at each frequency multiplied by a factor $k^{-\frac{1}{2}}$. Hence in the case of quadratic phase distortion as considered here, $n = \frac{1}{2}$ in (104).

Based on the above considerations, the power spectrum at any frequency ω for the above two limiting cases would vary with γ as indicated in Fig. 13. The shape of the curves between these two limiting cases would in a first approximation be represented by the function $H(\gamma)$ shown in Fig. 13.

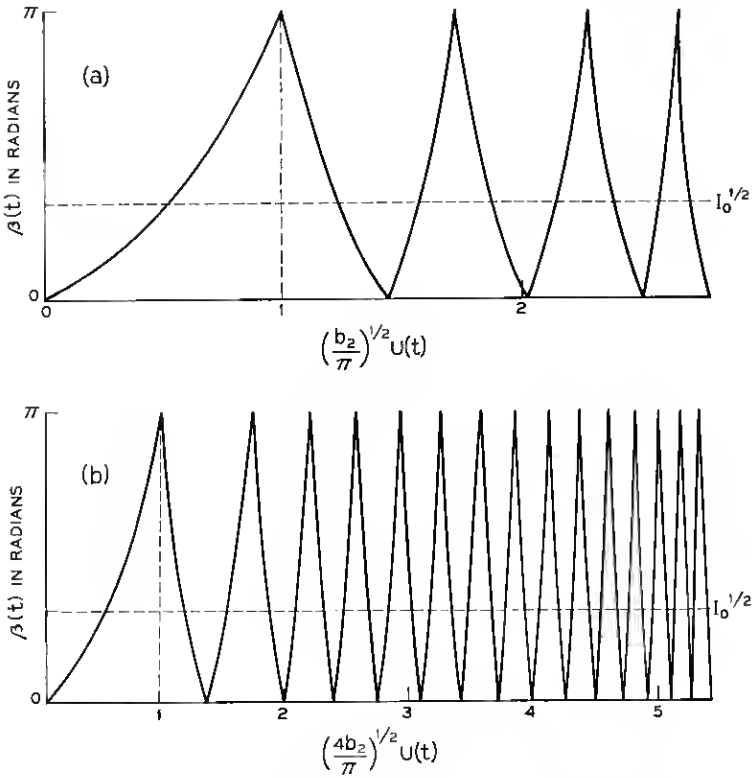

Fig. 14 — (*a*) Relation of instantaneous phase distortion $\beta(t)$ to instantaneous frequency deviation $u(t)$ for a given b_2; (*b*) relation of instantaneous phase distortion to instantaneous frequency deviation with fourfold increase in b_2.

A.10 *Approximation for* $\rho(\omega)$

The ratio $\rho(\omega)$ of intermodulation noise power in a narrow band at ω to average signal power in the same narrow band can be written

$$\rho(\omega) = \frac{2C(\omega)}{\mu^2} H(\gamma). \tag{106}$$

This relation differs from (94) in that $h(\gamma)$ as shown in Fig. 13 is replaced by $H(\gamma)$ shown in the same figure, and C is replaced by $C(\omega)$. The constant C defined through (74) depends on the frequency pre-emphasis $p(\omega)$. The function $C(\omega)$ depends both on the frequency pre-emphasis $p(\omega)$ and the frequency under consideration.

For the particular type of frequency pre-emphasis represented by

(60), expression (106) must conform with (61). This results in the following approximate relation

$$\rho(\omega) = \left(\frac{B}{D}\right)^2 G(c,a)H(\gamma) \tag{107}$$

where $H(\gamma)$ is the function shown in Fig. 13 and

$$G(c,a) = \frac{3a^2}{(1 + ca^2)(3 + c)} F(c,a) \tag{108}$$

where $F(c,a)$ is given by (62).

In the particular case in which $c = 16$ and $a = f/B = 1$

$$G(c,a) \approx 0.192 \tag{109}$$

and (107) yields

$$\rho(B) = \left(\frac{B}{D}\right)^2 \times 0.192H(\gamma) \tag{110}$$

$$= \left(\frac{B}{D}\right)^2 \times 0.192 \cdot \gamma^2 \quad \text{for} \quad \gamma \ll 1. \tag{111}$$

REFERENCES

1. Sunde, E. D., Digital Troposcatter Transmission and Modulation Theory, this issue, Part 1, p. 143.
2. Clutts, C. E., Kennedy, R. N., and Trecker, J. M., Results of Bandwidth Tests on the 185-Mile Florida-Cuba Scatter Radio Systems, IRE Trans. on Communication Systems, **9**, December, 1961, p. 434.
3. Beach, C. D., and Trecker, J. M., A Method for Predicting Interchannel Modulation Due to Multipath Propagation in FM and PM Tropospheric Radio Systems, B.S.T.J., **42**, January, 1963, p. 1.
4. Bennett, W. R., Curtis, H. E., and Rice, S. O., Interchannel Interference in FM and PM Systems under Noise Loading Conditions, B.S.T.J., **34**, May, 1955, p. 601.
5. Medhurst, R. G., and Small, G. F., Distortion in Frequency-Modulation Systems Due to Small Sinusoidal Variations of Transmission Characteristics, Proc. IRE, **44**, November, 1956, p. 1608.
6. Medhurst, R. G., and Small, G. F., An Extended Analysis of Echo Distortion in FM Transmission of Frequency-Division Multiplex, Proc. IEE, **103**, Pt. *B*, March, 1956, p. 190.
7. Carson, J. R., and Fry, T. C., Variable Frequency Electric Circuit Theory with Applications to the Theory of Frequency Modulation, B.S.T.J., **16**, October, 1937, p. 513.
8. van der Pohl, B., The Fundamental Principles of Frequency Modulation, Jour. IEE, Part III, May, 1946, p. 153.
9. Albersheim, W. J., and Schafer, J. P., Echo Distortion in the FM Transmission of Frequency Division Multiplex, Proc. IRE, **40**, March, 1952, p. 316.
10. Rice, S. O., Mathematical Analysis of Random Noise-I and -II, B.S.T.J., **23**, July, 1944, p. 282, and **24**, January, 1945, p. 46.
11. Rice, S. O., Distortion Produced by a Noise Modulated Signal by Nonlinear Attenuation and Phase Shift, B.S.T.J., **36**, July, 1957, p. 879.